Published in final edited form as:
Cancer Res. 2018 January 15; 78(2): 410–421. doi:10.1158/0008-5472.CAN-17-1153.

ER alpha binding by transcription factors NFIB and YBX1 enables FGFR2 signalling to modulate estrogen responsiveness in breast cancer

Thomas M. Campbell[1], **Mauro A. A. Castro**[2], **Kelin Gonçalves de Oliveira**[2], **Bruce A. J. Ponder**[1], and **Kerstin B. Meyer**[1,3,*]

[1]Cancer Research UK Cambridge Institute, University of Cambridge, Li Ka Shing Centre, Robinson Way, Cambridge CB2 0RE, UK

[2]Bioinformatics and Systems Biology Lab, Federal University of Paraná (UFPR), Polytechnic Center, Rua Alcides Vieira Arcoverde, 1225 Curitiba, PR 81520-260, Brazil

Abstract

Two opposing clusters of transcription factors (TFs) have been associated with the differential risks of estrogen receptor positive or negative breast cancers, but the mechanisms underlying the opposing functions of the two clusters are undefined. In this study, we identified NFIB and YBX1 as novel interactors of the estrogen receptor (ESR1). NFIB and YBX1 are both risk TF associated with progression of ESR1-negative disease. Notably, they both interacted with the ESR1-FOXA1 complex and inhibited the transactivational potential of ESR1. Moreover, signaling through FGFR2, a known risk factor in breast cancer development, augmented these interactions and further repressed ESR1 target gene expression. We therefore show that members of two opposing clusters of risk TFs associated with ESR1 positive and negative breast cancer can physically interact. We postulate that this interaction forms a toggle between two developmental pathways affected by FGFR2 signaling, possibly offering a junction to exploit therapeutically.

Keywords

Breast cancer; ESR1; NFIB; YBX1; FGFR2

Introduction

The estrogen receptor (ESR1) is the key driver and therapeutic target of breast cancer [1] and plays a critical role in determining the risk of developing this disease [2–4]. Using a systems biology approach we have examined transcriptional networks in breast cancer affecting ESR1 activity and have identified two distinct and opposing clusters of transcription factors (TFs) associated with enhanced breast cancer risk [5]. The “cluster 1” risk TFs are associated with estrogen receptor-positive (ER^+) breast cancer risk and comprise TFs such as ESR1, FOXA1 and GATA3 whereas the “cluster 2” risk TFs appear to

*Corresponding author: Kerstin.Meyer@sanger.ac.uk.
[3]Current address: Wellcome Trust Sanger Institute, Wellcome Genome Campus, Hinxton, Cambridge CB10 1SA, UK.

Europe PMC Funders Author Manuscripts

be associated with estrogen receptor-negative (ER^-), basal-like breast cancer (BLBC). Two of the TFs located in the cluster associated with ER^- disease are NFIB and YBX1. Here we examine the molecular mechanisms underlying the opposing functions of the two groups of TFs by studying protein-protein interactions between TFs and their functional consequences. We also examine the effect of cell signalling, in particular by fibroblast growth factor receptor 2 (FGFR2), on the relative activity of the two groups of TFs.

The nuclear factor I (NFI) family of TFs consists of four members, NFIA, NFIB, NFIC and NFIX, which can all bind DNA as homo- or heterodimers [6]. They are particularly important during developmental stages [7, 8], and NFIB is crucial for normal lung and brain development [9]. NFIB commonly has an increased copy number in small cell lung cancer (SCLC), indicating a role as an oncogene [10]. In BLBC, both copy number and expression levels of NFIB are also increased [11, 12]. In addition, NFIB is important in the regulation of expression of mammary gland-specific genes, specifically those associated with lactation such as Whey acidic protein (WAP) and α-lactalbumin [13]. NFIB has been shown to modulate androgen receptor (AR) target genes in prostate cancer cells via an interaction with FOXA1 [14, 15]. An investigation into whether similar modulation of estrogen receptor (ER) occurs in the breast has yet to be carried out.

Y-box binding protein 1 (YBX1) is a member of a family of DNA- and RNA-binding proteins with an evolutionarily ancient and conserved cold shock domain. It is a multifunctional protein that certainly does not follow the classical “one protein-one function” rule, but rather has disordered structure suggesting many different functions [16]. It has been extensively studied in cancer and its overexpression is associated with many hallmarks of the disease. It is expressed in many breast cancer cell lines regardless of subtype. However, there are higher levels of phosphorylated YBX1 in BLBC cell lines [17, 18]. YBX1 expression in inversely correlated with ER, PR and HER2 expression and is positively correlated with the MAPK signalling cascade, a pathway important in BLBC [19, 20]. YBX1 is highly expressed in 70% of BLBC cases and many of its target genes are associated with a basal-like signature [18, 20]. Higher expression of YBX1 correlates with poor survival, drug resistance and a high rate of relapse in all subtypes [18, 19, 21–23]. Suppression of YBX1 reduces 2D cell growth and growth in mammospheres [18, 20]. There is also evidence to suggest that YBX1 binds ESR1 in ER^+ breast cancer cell nuclei [24, 25].

A locus within the second intron of the FGFR2 (fibroblast growth factor receptor 2) gene is consistently identified as the genetic locus most strongly associated with estrogen receptor-positive (ER^+) breast cancer risk by independent genome-wide association studies (GWASs) [26]. We have shown previously that the top three risk single nucleotide polymorphisms (SNPs) [27, 28] act to reduce FGFR2 gene expression and enhance the estrogen response [29]. Increased FGFR2 stimulation repressed estrogen signalling in ER^+ breast cancer cell lines. However, the underlying molecular mechanism remains unclear.

Here, we demonstrate that two members of the cluster 2 TFs, NFIB and YBX1, both physically interact with ESR1, repress its activity, and drive breast cancer cells towards a less estrogen-dependent cancer phenotype. FGFR2 signalling augments this interaction and subsequent repression of ESR1 target gene expression. Our evidence suggests that FGFR2

has wide-ranging effects on driving breast cancer cells towards a more basal-like phenotype and that inhibiting FGFR2 signalling in ER^+ breast cancer sensitizes cells to anti-estrogen therapies.

Materials and Methods

Cell culture

MCF-7 human breast cancer cells and HeLa cells were cultured in DMEM (Invitrogen) supplemented with 10% FBS and antibiotics. ZR751 human breast cancer cells were cultured in RPMI (Invitrogen) supplemented with 10% FBS and antibiotics. SUM52PE human breast cancer cells were cultured in Ham/F-12 (Invitrogen) supplemented with 10% FBS, 5 μg/mL insulin, 1 μg/mL hydrocortisone and antibiotics. All cells were maintained at 37°C, 5% CO_2, obtained from the CRUK Cambridge Institute collection and authenticated by STR genotyping.

Quantitative RT-PCR

1 μg of total RNA was reverse transcribed using the High Capacity cDNA Reverse Transcription Kit (Applied Biosystems) and qRT-PCR performed using cDNA obtained from 10 ng of total RNA. qRT-PCR was performed using a QuantStudio6 system (Life Technologies). Amplification and detection were carried out in 384-well Optical Reaction Plates (Applied Biosystems) with Power SYBR Green Fast 2x qRT-PCR Mastermix (Applied Biosystems). All expression data were normalised to DGUOK expression. The specificity of primers (Supplementary Table 1) was confirmed through generation of single peaks in a melt-curve analysis. Data analysis was performed using the $2^{-\Delta\Delta CT}$ method [30].

Western immunoblotting

Cells were grown in 10 cm Petri dishes, washed in PBS and lysed on ice in RIPA buffer with cOmplete Mini EDTA-free protease inhibitor cocktail (Roche). Resulting cell lysates were passed through a fine-gauge syringe needle several times, centrifuged at 10,000 g for 1 minute and left at -80°C at least overnight. Protein samples were separated by SDS-PAGE using 4-12% Bis-Tris gels (Novex) for 2.5 hours (30 minutes at 60 V, 120 minutes at 120 V) and transferred by electrophoresis using an iBlot (Novex) for 7 minutes onto a nitrocellulose membrane (iBlot Gel Transfer Stacks; Novex). Successful transfer of protein was confirmed using Ponceau S Solution (Sigma). Membranes were “blocked” at room temperature for 1 hour with 5% dried milk in Tris-buffered saline (TBS) with 0.1% Tween-20 (TTBS), washed 3x with TTBS and probed with the relevant primary antibody (Supplementary Table 2) in blocking solution at 4°C overnight. Membranes were then re-washed with TTBS 3x and incubated with appropriate HRP-conjugated secondary antibody (Supplementary Table 2) in blocking solution at room temperature for 90 minutes. Following further washing with TTBS, blots were treated with SuperSignal West Chemiluminescent Substrate (Thermo Scientific) and immunoreactive proteins detected by exposure to film (FUJIFILM).

Rapid Immunoprecipitation Mass Spectrometry of Endogenous Proteins

Rapid Immunoprecipitation Mass Spectrometry of Endogenous Proteins (RIME) was performed on the ESR1 protein (ERα) in MCF-7 and ZR751 ER^+ breast cancer cells, as

described previously [31–33]. Briefly, cells were crosslinked for eight minutes at room temperature in media containing 1% formaldehyde. Crosslinking was quenched by adding glycine to a final concentration of 0.2 M. Cells were washed with ice-cold PBS, harvested in PBS, and the resulting cell pellet was washed in PBS. The nuclear fraction was extracted from the samples by first resuspending the pellet in 10 mL LB1 buffer (50 mM HEPES-KOH pH7.5, 140 mM NaCl, 1 mM EDTA, 10% glycerol, 0.5% NP-40, 0.25% Triton X-100) for 10 minutes at 4°C. Cells were then pelleted, resuspended in 10 mL LB2 buffer (10 mM Tris-HCl pH8.0, 200 mM NaCl, 1 mM EDTA, 0.5 mM EGTA) and mixed at 4°C for five minutes. Cells were then pelleted and resuspended in 300 μL of LB3 buffer (10 mM Tris-HCl pH8.0, 100 mM NaCl, 1 mM EDTA, 0.5 mM EGTA, 0.1% Na-deoxycholate, 0.5% N-lauroylsarcosine) and sonicated in a waterbath sonicator (Diagenode). The resulting supernatant was incubated with protein A Dynabeads (Invitrogen) prebound with ESR1 antibody (Santa Cruz sc-543 X), and immunoprecipitation was performed at 4°C overnight. The beads were washed 10x in RIPA buffer and twice in 100 mM AMBIC solution. Tryptic digestion of bead-bound protein and mass spectrometry was performed by the Proteomics Core Facility at The CRUK Cambridge Institute using an LTQ Velos-Orbitrap MS (Thermo Scientific) coupled to an Ultimate RSLCnano-LC system (Dionex). Full RIME data are given in Supplementary Table 3.

Co-immunoprecipitation

Cells from five 15 cm Petri dishes were harvested after washing with PBS. The cellular nuclear fraction was then obtained using a nuclear extraction kit (Affymetrix), according to manufacturer's protocol. The resulting nuclear fraction was precleared for 60 minutes with protein A Dynabeads (Invitrogen). Immunoprecipitation (IP) was then performed with 5 μg of antibody prebound to protein A Dynabeads. Each IP was coupled with a corresponding IgG-negative control of the same species. IP was performed overnight and the beads were washed with wash buffer (50 mM Tris pH7.4, 140 nM NaCl, 2 mM EGTA, 0.1% Tween-20). Beads were then boiled at 95°C for 15 minutes in LDS loading buffer and Western immunoblot analysis performed.

Molecular Cloning

The plasmid constructs used for the fluorescence resonance energy transfer (FRET) were developed as follows from mCerulean3 (mCer3)-C1 and mVenus-C1 vectors kindly donated by Magdalena Grabowska [14]. The ESR1-Cerulean construct was created by amplifying the gene encoding ESR1 (from RC213277; OriGene) and performing sequential digestion/ligation of the product and mCer3-C1 vector using NheI and AgeI restriction enzymes. The NFIB/YBX1-Cerulean and NFIB/YBX1-Venus constructs were created similarly (from plasmids RC231275 (NFIB) and RC209835 (YBX1); OriGene). The FOXA1-Venus construct was kindly donated by Magdalena Grabowska [14]. All primer sequences are given in Supplementary Table 4. The orientation and sequence of all plasmids were confirmed by DNA sequencing (GATC Biotech).

Fluorescence resonance energy transfer

HeLa cells were transiently transfected with plasmid DNA encoding the tagged TFs described above. 15,000 cells were seeded into each well of a μ-Slide 8 Well chambered

coverslip (ibidi) and cultured for 24-48 hours. Samples were then fixed with 4% paraformaldehyde for 20 minutes at room temperature, washed in PBS, and stored in PBS. FRET imaging was performed using a Leica TCS SP5 confocal microscope (Leica Microsystems). Data were analysed by FRET Acceptor Photobleaching [34] using the Leica LAS imaging software (Leica Microsystems). A total of 20-30 cells/well were quantified for FRET efficiency, and the experiments were repeated in at least three cellular preparations. FRET efficiency was calculated as follows:

$$\text{Efficiency} = \frac{Donor_{post-bleach} - Donor_{pre-bleach}}{Donor_{post-bleach}}$$

Luciferase reporter assay

MCF-7 cells stably expressing a luciferase reporter gene under the transcriptional control of an upstream ESR1 and FOXA1 binding site, cloned from the human RARα gene (kindly donated by the lab of Jason Carroll), were plated at 50,000 cells/well in 24-well dishes and left in complete medium until 50-70% confluent. Cells were then transfected with the relevant siRNA/expression plasmids and a β-galactosidase construct using FuGENE HD Transfection Reagent (Promega), according to manufacturer's protocol (DNA:FuGENE ratio = 1 μg:4 μl). After 24 hours at 37°C, 5% CO_2, cells were lysed with Reporter Lysis Buffer (Promega) and luciferase and β-galactosidase assays were performed on a PHERAstar FS Microplate Reader (BMG LABTECH) using the appropriate assay kits (Promega), according to manufacturer's protocol. Each assay was performed in triplicate and a total of three assays were performed on three separate days.

Transient transfection of siRNA

MCF-7 cells were transfected with ON-TARGETplus SMARTpool siRNA (Dharmacon) directed against ESR1 (L-003401-00), FOXA1 (L-010319-00), NFIB (L-008456-00), YBX1 (L-010213-00), FGFR2 (L-003132-00), and a control non-targeting pool (D-001810-10) using Lipofectamine RNAiMax Reagent (Invitrogen), according to manufacturer's protocol. Following addition of the transfection complexes, cells were incubated at 37°C, 5% CO_2 for at least 24 hours before experiments were performed.

Transient transfection of plasmid DNA

Cells were plated at 50,000 cells/well in 24-well dishes and grown in complete medium until 50-70% confluent, transiently transfected with plasmid using FuGENE HD Transfection Reagent (Promega), according to manufacturer's protocol (DNA:FuGENE ratio = 1 μg:4 μl), and maintained for 24–48 hours at 37°C, 5% CO_2 in complete medium prior to conducting experiments.

Generation of stable cell lines

MCF-7 cells stably expressing FLAG-tagged NFIB (RC231275; OriGene) and YBX1 (RC209835; OriGene) were generated via transfection of the NFIB and YBX1 constructs, as described above. The day following cell transfection, cell culture medium was changed to fresh medium containing 1.5 mg/mL geneticin (G418; Invitrogen). Cells were grown and

passaged, with media changed every other day until mass cell death was observed. Clonal populations of cells were selected by transferring well-isolated single clumps of cells into a 24-well plate. Cells were expanded under antibiotic selection.

Proliferation assay

Cells were plated at 4000 cells per well into 96-well plates and cell numbers monitored in real time by *in vitro* micro-imaging using an IncuCyte incubator (Essen BioScience), allowing for monitoring of cell proliferation by observing cell confluence. Images were taken every three hours and data consisted of an average of four separate images taken for each well. Assays were performed in eight separate wells on three separate occasions.

RNA collection and RNA sequencing

Total RNA was extracted from cells using the miRNeasy Mini Kit (QIAGEN) and quality checked using an RNA 6000 Nano Chip on a 2100 Bioanalyser (Agilent). mRNA-seq libraries were prepared from three biological replicates of each stable overexpression system using the TruSeq Stranded mRNA Library Prep Kit (Illumina), according to manufacturer's protocol. Single-end 50 bp reads generated on the Illumina HiSeq 4000 were aligned to the human genome version GRCh37.75. Read counts were then obtained using Subread v1.5.1 [35], normalised and tested for differential gene expression using the Bioconductor package DESeq2 [36, 37]. Multiple testing correction was applied using the Benjamini-Hochberg method. The full mRNA-seq data set has been deposited in GEO under accession GSE95299.

Two-tailed gene set enrichment analysis

Two-tailed gene set enrichment analysis (GSEA) [38] was performed as described previously [29]. *P* values derived from DESeq analyses of the mRNA-seq data were $-\log_{10}$ transformed and then signed according to whether genes were up- or down-regulated compared with control samples. These values were then used for ranking and weighting of genes in subsequent GSEA analyses.

Survival analysis

Analysis of breast cancer patient survival stratified by YBX1 expression was carried out using the KM plotter [39].

Patient-derived xenograft (PDX) analysis

A subset of breast cancer samples from Novartis' PDX dataset [40] was stratified according to YBX1, NFIB and FGFR2 expression levels. Clinical tamoxifen response was assessed by comparison of tumour volume between treated versus untreated groups. *P* values were generated with Repeated Measures one-way ANOVA (RM-ANOVA) statistical test. ESR1 gene expression levels were also compared between groups using Kruskal-Wallis.

Stimulation of FGFR2 signalling

Cells in which FGFR2 signalling was stimulated were first left in complete medium overnight. Cell synchronisation via estrogen-starvation was then carried out for three days in

estrogen-free media (phenol red-free media supplemented with 5% charcoal dextran-treated FBS and 2 mM L-glutamine), with media changes every 24 hours. Estrogen-deprived cells were stimulated with 1 nM β-estradiol (E2; Sigma) or 100 ng/mL FGF10 (Invitrogen) in combination with 1 nM E2, for 6 hours.

Results

ESR1 interacts with NFIB and YBX1

Previously, we have shown that FGFR2 signalling reduces estrogen responsiveness in breast cancer cells [29] but has little effect on ESR1 expression levels. We therefore tested whether FGFR2 signalling affects the interaction of ESR1 with its protein binding partners. To this end, we performed a Rapid Immunoprecipitation Mass Spectrometry of Endogenous Proteins (RIME) analysis on the ESR1 protein (Table 1). Unique peptides for ESR1, as well as its known binding partners, FOXA1 and GATA3, were detected. The only other cluster 1 or 2 TFs for which unique peptides were detected in the RIME analysis were NFIB and YBX1. YBX1 has previously been reported to interact with ESR1 [24, 25], whereas NFIB appears to be a novel interacting partner. RIME cannot be considered a truly quantitative technique. Nevertheless, the number of unique peptides for NFIB and YBX1 detected by mass spectrometry increases when both MCF-7 and ZR751 are stimulated with FGF10, the most potent agonist of the FGFR2 receptor [41, 42]. This suggests that FGFR2 signalling in ER^+ breast cancer cell lines might augment the interaction of ESR1 with the two cluster 2 risk TFs.

To confirm the exploratory RIME experiments, co-immunoprecipitation experiments were performed in order to test if NFIB and YBX1 could be confirmed as ESR1 binding partners by Western immunoblotting. Following immunoprecipitation of the nuclear fraction of both MCF-7 and ZR751 cells with an ESR1 antibody (Figure 1A), ESR1, FOXA1 and GATA3 protein bands could be resolved by Western immunoblotting, as expected. Moreover, NFIB and YBX1 were also present in the ESR1 immunoprecipitates, whilst being absent in the IgG control pull-downs, suggesting that both NFIB and YBX1 physically interact with the ESR1 protein in the nucleus of these ER^+ breast cancer cells. As control experiments, blots were also performed for TFs that are not expected to bind to ESR1 (E2F2, SP1 and YY1), and no protein bands were detected. The inverse pull-down experiments were also performed, in which the nuclear fractions of MCF-7 and ZR751 cells were immunoprecipitated with an NFIB (Figure 1B) or YBX1 (Figure 1C) antibody. In both cases the ESR1 protein was detected in the immunoprecipitate.

RIME data suggested that FGFR2 signalling in MCF-7 and ZR751 cells might increase the association of ESR1 with both NFIB and YBX1. Therefore, co-immunoprecipitation experiments were also carried out in MCF-7 cells that had been stimulated with estrogen alone or with a combination of estrogen and FGF10 (Figure 1D,E). Densitometry analysis of the Western immunoblots against NFIB and YBX1 following pull-down of ESR1 shows that stimulation of MCF-7 cells with FGF10 appears to augment the interaction of the two ER^- risk TFs with ESR1, without affecting protein levels (Figure 1F,G). Moreover, FGFR2 signalling in ER^+ breast cancer cells increases the level of phosphorylated YBX1 (demonstrated in MCF-7 cells), whilst FGFR2 inhibition reduces it (demonstrated in

SUM52PE cells, which carry an FGFR2 gene amplification) (Figure 1H,I). Our finding that YBX1 can bind to ESR1 is consistent with recent reports of an interaction between these two proteins [24, 25].

Fluorescence resonance energy transfer (FRET), which is facilitated by tagging proteins of interest with fluorescent proteins as reporters, is an imaging technique useful for studying protein-protein interactions [43]. FRET only occurs when the fluorescent proteins are within very close proximity of each other (<10 nm), thereby allowing for the measurement of the proximity of proteins of interest (Figure 2A). Here, we tagged FOXA1, NFIB, YBX1 and ESR1 with either a donor (mCerulean3) or acceptor (mVenus) fluorescent protein and performed FRET in HeLa cells expressing the constructs (Figure 2B; Supplementary Figure 1). Consistent with previous reports of ESR1 and FOXA1 interactions [44], cotransfected ESR1-Cer and FOXA1-Venus emitted a strong FRET signal (Figure 2B) with an efficiency of 0.139 ± 0.011 (Supplementary Figure 2). To determine whether NFIB and FOXA1 are also able to interact directly, cells were cotransfected with NFIB-Cer donor and FOXA1-Venus acceptor constructs. The pairing resulted in a positive FRET signal with a FRET efficiency of 0.055 ± 0.007. On the other hand, the ESR1-Cer and NFIB-Venus pairing did not result in FRET (efficiency of 0), suggesting that these proteins do not interact directly. To test the hypothesis that FOXA1 can bridge the interaction between ESR1 and NFIB, we cotransfected cells with ESR1-Cer, NFIB-Venus and untagged FOXA1. The FRET efficiency of ESR1-Cer and NFIB-Venus was increased to 0.018 ± 0.003. This result suggests that FOXA1 serves as an intermediary “bridge” to bring ESR1 and NFIB together. The same experiments were carried out with YBX1 FRET constructs, demonstrating that YBX1 is able to bind to ESR1 directly, without requiring FOXA1 (Figure 2B; Supplementary Figure 2).

NFIB and YBX1 suppress ESR1 activity

Having established that both NFIB and YBX1 interact with the ESR1/FOXA1 TF complex, we asked whether NFIB and YBX1 are able to influence the transcriptional activity of ESR1. When NFIB or YBX1 were transiently overexpressed in MCF-7 cells, expression of the ESR1-target gene, pS2, was significantly reduced compared with the control cells (Figure 3A). Conversely, reduction of NFIB or YBX1 levels via siRNA transfection resulted in increased pS2 expression. The same results were also obtained for other ESR1-target genes (Supplementary Figure 3). Similarly, when NFIB or YBX1 were transiently overexpressed in MCF-7 cells stably expressing a luciferase reporter gene under the transcriptional control of an upstream ESR1/FOXA1 binding site, luciferase expression was significantly reduced compared with control cells (Figure 3B). These data suggest that both NFIB and YBX1 are able to inhibit ESR1-mediated transcriptional activity.

To investigate further the possible role of NFIB and YBX1 on ESR1 activity, MCF-7 cell lines stably overexpressing FLAG-tagged NFIB or YBX1 were generated (Supplementary Figure 4). For each TF three independent clones were expanded, mRNA-seq data generated and the regulatory network examined. We previously defined regulons (set of target genes) for all TFs by measuring the similarities in gene expression patterns of the TF of interest and all possible target genes in gene expression data from breast tumour samples [5]. Here, we

carried out a two-tailed GSEA [5, 29] to assay the activity of the ESR1 regulon in the stably transfected cells. As a control we show the behaviour of the ESR1 regulon in response to estrogen stimulation. As expected, positive targets of ESR1 are induced and negative targets of ESR1 are repressed in the parental MCF-7 cells (Figure 4A). Overexpression of both NFIB and YBX1 leads to a relative repression of the ESR1 regulon (Figure 4B,C), with negative ESR1 targets being upregulated and positive targets showing lower expression. These experiments confirm that both NFIB and YBX1 are able to inhibit ESR1 function.

When the MCF-7 cells stably overexpressing NFIB or YBX1 were estrogen-starved, they were able to proliferate faster than estrogen-starved parental MCF-7 cells (Figure 4D,E). A study by Shibata *et al.* reported that YBX1 is able to reduce the stability of ESR1 protein [25]. However, Western immunoblots of cell extracts demonstrate that full length ESR1 protein levels are not altered by either NFIB or YBX1 overexpression in our system (Supplementary Figure 4). Our results suggest that overexpression of these cluster 2 risk TFs is able to drive ER^+ breast cancer cells towards a more ER^-, basal-like cancer phenotype in which estrogen-dependency is reduced.

FGFR2 signalling and breast cancer regulon activity

To further assess the shift from luminal to a more basal-like phenotype we extended our two-tailed GSEA to all regulons and visualised the results in a tree and leaf diagram, where regulons are represented as leaves and the branching between them is a measure of their relatedness [5]. Using this approach, a gene signature derived from ER^+ versus ER^- tumours showed a positive enrichment in the regulons of cluster 1 risk TFs and a negative enrichment of cluster 2 risk TFs (Figure 5A). A basal gene signature showed the inverse (Figure 5B). Interestingly, we found that a FGFR2 signalling gene signature was able to activate the NFIB and YBX1 regulons, as well as almost all TF regulons that are associated with ER^- disease (Figure 5C), mimicking very closely the results obtained with the basal gene signature. A reduction of FGFR2 gene expression via siRNA transfection has the opposite effect, increasing the activity of ESR1 and other cluster 1 TFs (Figure 5D), supporting and extending our earlier findings that FGFR2 signalling opposes estrogen signalling.

The fact that FGFR2 signalling inhibits estrogen signalling in ER^+ breast cancer cells, possibly via an increased association of ESR1 with the ER^- risk TFs, NFIB and YBX1, led us to test the hypothesis that the inhibition of FGFR2 signalling in ER^+ breast cancer cells sensitizes cells to anti-estrogen therapies. When three different ER^+ breast cancer cell lines (MCF-7, ZR751 and T47D), which all express NFIB and YBX1 (Figure 6A), are treated with the FGFR2 inhibitors, AZD4547 and PD173074, their growth, as measured in an IncuCyte incubator, is more sensitive to the anti-estrogen tamoxifen (Figure 6B-D; Supplementary Figure 5). This suggests that anti-FGFR2 treatments make breast cancer cells more reliant on estrogen signalling for growth, and could therefore be used in combination with anti-estrogen therapies to treat breast cancer. When MCF-7 cells stably overexpressing either NFIB or YBX1 are treated with siRNA against NFIB/YBX1, they become significantly less sensitive to the combined drug treatment when compared to non-transfected control cells (Figure 6E,F; Supplementary Figure 5), suggesting that NFIB and YBX1 do indeed play an important role in the FGFR2-driven estrogen activity/sensitivity of

breast cancer cells. Much more work is needed to determine if the effect of FGFR2 signalling on a breast cancer cell's reliance on estrogen signalling is primarily mediated by NFIB and YBX1. However, it is interesting to note that overexpression of YBX1 in breast cancer is associated with poorer survival, even when tested just in ER^+ breast cancer (Supplementary Figure 6). Furthermore, in patient-derived xenograft (PDX) models of breast tumours [40] we find that tamoxifen treatment is not very effective in PDXs with high YBX1 expression (Supplementary Figure 7), although this group is likely to contain ER^- tumours. In contrast, tamoxifen efficacy is greater in YBX1-low PDXs and even greater in PDXs that express both low FGFR2 and YBX1, further supporting the notion that inhibition of FGFR2 may increase a tumour's response to tamoxifen.

Discussion

In this study we demonstrate that in ER^+ breast cancer the TFs NFIB and YBX1 interact with ESR1, the key driver of luminal breast cancer. We examine the functional consequences of this interaction and find that NFIB and YBX1 are each able to repress transcriptional activation by ESR1. This can be observed in reporter assays, at the level of endogenous estrogen-regulated genes such as pS2, and also in the reduction of the overall activity of the ESR1 regulon. The interaction between YBX1 and ESR1 is direct, whilst NFIB requires FOXA1 as a bridging protein that allows the interaction. The complex formation we observe between NFIB or YBX1 and ESR1 may explain the opposing action that NFIB/YBX1 and ESR1 have on shared target genes [5]. In addition to repressing ESR1, NFIB and YBX1 are also able to drive proliferation: whilst proliferation of parental MCF-7 cells is strictly dependent on the presence of estrogen and hence nuclear ESR1, MCF-7 cells overexpressing either NFIB or YBX1 are able to grow in estrogen-depleted medium.

To date, NFIB and YBX1 have primarily been associated with ER^- breast cancer, where both factors contribute to increased aggressiveness and metastatic potential [12, 45]. We now report that these two TFs repress ESR1 activity, suggesting that they may play a similar role in ER^+ breast cancer. Although ER^+ breast cancer has better patient outcomes, in large part driven by the effectiveness of hormone deprivation therapy, relapse and resistance to therapy are relatively common and can occur many years after the primary tumour was diagnosed and treated [46]. Our previous work suggests that patient outcomes are strongly affected by the relative activity of TFs driving ER^+ (cluster 1, e.g. ESR1, GATA3, FOXA1) versus ER^- disease (cluster 2, e.g. YBX1, NFIB). We found that, in an ER^+ patient cohort, patients with a repressed ESR1 regulon have worse prognosis [5]. We now show that NFIB and YBX1 can both function to repress the activity of the ESR1 regulon. In line with this observation, we found that in clinical samples from patients with ER^+ disease, higher YBX1 expression is associated with reduced survival. As a corollary, interventions that increase the activity of the ESR1 regulon may improve patient outcomes, since the tumour is likely to have increased sensitivity to estrogen deprivation therapy.

We have previously demonstrated that the risk gene FGFR2 can influence the way in which a cell responds to estrogen, with FGFR2 signalling leading to reduced activity of the ESR1 regulon [29]. We have now extended our analysis and found that FGFR2 signalling not only affects the ESR1 regulon, but alters the activity of many TFs: the activity of TFs highly

expressed in luminal A or B tumours is decreased, whilst the activity of TFs highly expressed in basal-like breast cancer, such as NFIB and YBX1, is increased. A link between FGFR2 signalling and the activity of specific TFs has previously been reported. For example, in MCF-7 cells it causes degradation of the progesterone receptor, leading to increased proliferation and cell migration [47]. FGFR2 mediated activation of TFs associated with ER^- disease has not been studied directly, but indirect evidence exists. Signalling through FGFR2 leads to phosphorylation of RSK2, a mediator of anchorage independent growth and motility [48], which in turn activates YBX1 by phosphorylation [49]. Our data here indicates that FGFR2 signalling also increases the affinity of YBX1 for ESR1. Taken together these observations suggest that FGFR2 signalling increases the ability of YBX1 to activate target genes associated with BLBC, while at the same time increasing its ability to repress ESR1 target genes.

A role for FGFR2 in promoting a basal-like phenotype is consistent with previous findings. Functional studies of FGFR2 risk variants have demonstrated that a decrease in FGFR2 expression is associated with an increased risk in ER^+, but not ER^- breast cancer [28]. Conversely, FGFR2 amplifications, although infrequent (4%) [50], occur primarily in ER^- breast cancer. ER^- breast cancer cell lines tend to express higher levels of FGFR2 than ER^+ breast cancer cell lines [51] and are more sensitive to FGFR2 inhibitors such as PD173074. In clinical samples FGFR2 expression was higher in ER^- tumours and associated with poor patient outcome [51]. However, inhibition of FGFR2 signalling may also be effective in ER^+ tumours. We hypothesised that inhibition of FGFR2 signalling would make cells more dependent on estrogen (through upregulation of the ESR1 regulon) and therefore more sensitive to estrogen deprivation therapy. We tested this in cell lines and found that MCF-7, ZR751 and T47D cells treated with the FGFR2 inhibitors PD173074 or AZD4547 became more sensitive to treatment with tamoxifen.

FGFR inhibitors have been used effectively in the treatment of a variety of cancers, particularly those carrying FGFR amplifications [52, 53]. In breast cancer, the FGFR1 gene is amplified in about 13% of all breast cancer cases, whilst other FGFR genes are only rarely amplified (FGFR2, 1.5%; FGFR3, 0.5%; FGFR4, 1.5%) and are not frequently mutated. In line with our findings for FGFR2, activation of both FGFR1 (by amplification) and FGFR3 (*in vitro*) is associated with a reduced response to endrocrine therapy [54, 55]. This suggested clinical trials of FGFR inhibitors in combination with estrogen deprivation therapy. Not surprisingly, such trials have focussed on patients with amplifications in the FGFR pathway and gave encouraging results, but were ultimately inconclusive due to the small number of patients carrying the relevant genomic alteration [56]. Our work here suggests that rather than just focussing on FGFR amplification, alternative biomarkers such as the presence of activated YBX1 could be used to select patients that may benefit from FGFR2 inhibition. Consistent with this suggestion we find that high expression of YBX1 in ER^+ disease is associated with worse outcome. In the future this link needs to be further explored and activated YBX1 protein measured in ER^+ tumour samples. Alternatively, treatment could be focussed on downstream events, preventing the interaction of YBX1 or NFIB with ESR1. If this interaction is dependent on post-translational modifications, the inhibition of the relevant enzymes may be effective. As a first step towards moving our findings to the clinic we envisage the use of PDX models of breast cancer to confirm

Europe PMC Funders Author Manuscripts

synergy between FGFR2 inhibition and estrogen deprivation treatment in preventing tumour growth.

In conclusion, we demonstrate that signalling by FGFR2 pushes cells towards a more basal phenotype, which is at least in part mediated by facilitating the interaction between NFIB and YBX1, and ESR1. The regulatory loop between NFIB/YBX1 and ESR1 may be a promising target for developing new therapeutic strategies.

Supplementary Material

Refer to Web version on PubMed Central for supplementary material.

Acknowledgements

This work was funded by The Breast Cancer Research Foundation (BCRF) and by Cancer Research UK (CRUK). We thank the Genomics, Proteomics, Bioinformatics, Light Microscopy and Research Instrumentation Core Facilities at The CRUK Cambridge Institute for their help and expertise. We are grateful to Magdalena Grabowska for the gift of plasmids for the FRET experiments, and Kelly Holmes for the gift of the luciferase reporter cell line. B.A.J.P is a Gibb Fellow of CRUK.

References

1. Jia M, Dahlman-Wright K, Gustafsson JA. Estrogen receptor alpha and beta in health and disease. Best practice & research Clinical endocrinology & metabolism. 2015; 29(4):557–568. [PubMed: 26303083]
2. Clemons M, Goss P. Estrogen and the risk of breast cancer. The New England journal of medicine. 2001; 344(4):276–285. [PubMed: 11172156]
3. Advani P, Moreno-Aspitia A. Current strategies for the prevention of breast cancer. Breast cancer (Dove Medical Press). 2014; 6:59–71. [PubMed: 24833917]
4. Ban KA, Godellas CV. Epidemiology of breast cancer. Surgical oncology clinics of North America. 2014; 23(3):409–422. [PubMed: 24882341]
5. Castro MA, de Santiago I, Campbell TM, Vaughn C, Hickey TE, Ross E, et al. Regulators of genetic risk of breast cancer identified by integrative network analysis. Nature genetics. 2016; 48(1):12–21. [PubMed: 26618344]
6. Kruse U, Sippel AE. Transcription factor nuclear factor I proteins form stable homo- and heterodimers. FEBS Lett. 1994; 348(1):46–50. [PubMed: 8026582]
7. Campbell CE, Piper M, Plachez C, Yeh YT, Baizer JS, Osinski JM, et al. The transcription factor Nfix is essential for normal brain development. BMC Dev Biol. 2008; 8:52. [PubMed: 18477394]
8. Qian F, Kruse U, Lichter P, Sippel AE. Chromosomal localization of the four genes (NFIA, B, C, and X) for the human transcription factor nuclear factor I by FISH. Genomics. 1995; 28(1):66–73. [PubMed: 7590749]
9. Steele-Perkins G, Plachez C, Butz KG, Yang G, Bachurski CJ, Kinsman SL, et al. The transcription factor gene Nfib is essential for both lung maturation and brain development. Mol Cell Biol. 2005; 25(2):685–698. [PubMed: 15632069]
10. Dooley AL, Winslow MM, Chiang DY, Banerji S, Stransky N, Dayton TL, et al. Nuclear factor I/B is an oncogene in small cell lung cancer. Genes & development. 2011; 25(14):1470–1475. [PubMed: 21764851]
11. Han W, Jung EM, Cho J, Lee JW, Hwang KT, Yang SJ, et al. DNA copy number alterations and expression of relevant genes in triple-negative breast cancer. Genes, chromosomes & cancer. 2008; 47(6):490–499. [PubMed: 18314908]
12. Moon HG, Hwang KT, Kim JA, Kim HS, Lee MJ, Jung EM, et al. NFIB is a potential target for estrogen receptor-negative breast cancers. Molecular oncology. 2011; 5(6):538–544. [PubMed: 21925980]

13. Murtagh J, Martin F, Gronostajski RM. The Nuclear Factor I (NFI) gene family in mammary gland development and function. Journal of mammary gland biology and neoplasia. 2003; 8(2):241–254. [PubMed: 14635798]
14. Grabowska MM, Elliott AD, DeGraff DJ, Anderson PD, Anumanthan G, Yamashita H, et al. NFI transcription factors interact with FOXA1 to regulate prostate-specific gene expression. Molecular endocrinology (Baltimore, Md). 2014; 28(6):949–964.
15. Grabowska MM, Kelly SM, Reese AL, Cates JM, Case TC, Zhang J, et al. Nfib regulates transcriptional networks that control the development of prostatic hyperplasia. Endocrinology. 2015 en20151312.
16. Lyabin DN, Eliseeva IA, Ovchinnikov LP. YB-1 protein: functions and regulation. Wiley Interdiscip Rev RNA. 2014; 5(1):95–110. [PubMed: 24217978]
17. Bergmann S, Royer-Pokora B, Fietze E, Jurchott K, Hildebrandt B, Trost D, et al. YB-1 provokes breast cancer through the induction of chromosomal instability that emerges from mitotic failure and centrosome amplification. Cancer Res. 2005; 65(10):4078–4087. [PubMed: 15899797]
18. Finkbeiner MR, Astanehe A, To K, Fotovati A, Davies AH, Zhao Y, et al. Profiling YB-1 target genes uncovers a new mechanism for MET receptor regulation in normal and malignant human mammary cells. Oncogene. 2009; 28(11):1421–1431. [PubMed: 19151767]
19. Dahl E, En-Nia A, Wiesmann F, Krings R, Djudjaj S, Breuer E, et al. Nuclear detection of Y-box protein-1 (YB-1) closely associates with progesterone receptor negativity and is a strong adverse survival factor in human breast cancer. BMC Cancer. 2009; 9:410. [PubMed: 19930682]
20. Davies AH, Reipas KM, Pambid MR, Berns R, Stratford AL, Fotovati A, et al. YB-1 transforms human mammary epithelial cells through chromatin remodeling leading to the development of basal-like breast cancer. Stem Cells. 2014; 32(6):1437–1450. [PubMed: 24648416]
21. Habibi G, Leung S, Law JH, Gelmon K, Masoudi H, Turbin D, et al. Redefining prognostic factors for breast cancer: YB-1 is a stronger predictor of relapse and disease-specific survival than estrogen receptor or HER-2 across all tumor subtypes. Breast Cancer Res. 2008; 10(5):R86. [PubMed: 18925950]
22. Huang J, Tan PH, Li KB, Matsumoto K, Tsujimoto M, Bay BH. Y-box binding protein, YB-1, as a marker of tumor aggressiveness and response to adjuvant chemotherapy in breast cancer. Int J Oncol. 2005; 26(3):607–613. [PubMed: 15703814]
23. Maciejczyk A, Szelachowska J, Ekiert M, Matkowski R, Halon A, Lage H, et al. Elevated nuclear YB1 expression is associated with poor survival of patients with early breast cancer. Anticancer Res. 2012; 32(8):3177–3184. [PubMed: 22843890]
24. Tarallo R, Bamundo A, Nassa G, Nola E, Paris O, Ambrosino C, et al. Identification of proteins associated with ligand-activated estrogen receptor alpha in human breast cancer cell nuclei by tandem affinity purification and nano LC-MS/MS. Proteomics. 2011; 11(1):172–179. [PubMed: 21182205]
25. Shibata T, Watari K, Izumi H, Kawahara A, Hattori S, Fukumitsu C, et al. Breast Cancer Resistance to Antiestrogens Is Enhanced by Increased ER Degradation and ERBB2 Expression. Cancer research. 2017; 77(2):545–556. [PubMed: 27879270]
26. Fachal L, Dunning AM. From candidate gene studies to GWAS and post-GWAS analyses in breast cancer. Current opinion in genetics & development. 2015; 30:32–41. [PubMed: 25727315]
27. Edwards SL, Beesley J, French JD, Dunning AM. Beyond GWASs: illuminating the dark road from association to function. American journal of human genetics. 2013; 93(5):779–797. [PubMed: 24210251]
28. Meyer KB, O'Reilly M, Michailidou K, Carlebur S, Edwards SL, French JD, et al. Fine-scale mapping of the FGFR2 breast cancer risk locus: putative functional variants differentially bind FOXA1 and E2F1. American journal of human genetics. 2013; 93(6):1046–1060. [PubMed: 24290378]
29. Campbell TM, Castro MA, de Santiago I, Fletcher MN, Halim S, Prathalingam R, et al. FGFR2 risk SNPs confer breast cancer risk by augmenting oestrogen responsiveness. Carcinogenesis. 2016; 37(8):741–750. [PubMed: 27236187]
30. Livak KJ, Schmittgen TD. Analysis of relative gene expression data using real-time quantitative PCR and the 2(-Delta Delta C(T)) Method. Methods. 2001; 25(4):402–408. [PubMed: 11846609]

31. Mohammed H, Carroll JS. Approaches for assessing and discovering protein interactions in cancer. Molecular cancer research: MCR. 2013; 11(11):1295–1302. [PubMed: 24072816]
32. Mohammed H, D'Santos C, Serandour AA, Ali HR, Brown GD, Atkins A, et al. Endogenous purification reveals GREB1 as a key estrogen receptor regulatory factor. Nature protocols. 2013; 3(2):342–349.
33. Mohammed H, Taylor C, Brown GD, Papachristou EK, Carroll JS, D'Santos CS. Rapid immunoprecipitation mass spectrometry of endogenous proteins (RIME) for analysis of chromatin complexes. Cell reports. 2016; 11(2):316–326.
34. Gastard, M. FRET acceptor photobleaching (AB) in LASAF. 2006. Available from: http://bticornelledu/wp-content/uploads/2014/04/AppNote_FRET_ABpdf
35. Liao Y, Smyth GK, Shi W. The Subread aligner: fast, accurate and scalable read mapping by seed-and-vote. Nucleic acids research. 2013; 41(10):e108. [PubMed: 23558742]
36. Anders S, Huber W. Differential expression analysis for sequence count data. Genome biology. 2010; 11(10):R106. [PubMed: 20979621]
37. Love MI, Huber W, Anders S. Moderated estimation of fold change and dispersion for RNA-seq data with DESeq2. Genome biology. 2014; 15(12):550. [PubMed: 25516281]
38. Subramanian A, Tamayo P, Mootha VK, Mukherjee S, Ebert BL, Gillette MA, et al. Gene set enrichment analysis: a knowledge-based approach for interpreting genome-wide expression profiles. Proceedings of the National Academy of Sciences of the United States of America. 2005; 102(43):15545–15550. [PubMed: 16199517]
39. Gyorffy B, Lanczky A, Eklund AC, Denkert C, Budczies J, Li Q, et al. An online survival analysis tool to rapidly assess the effect of 22,277 genes on breast cancer prognosis using microarray data of 1,809 patients. Breast cancer research and treatment. 2010; 123(3):725–731. [PubMed: 20020197]
40. Gao H, Korn JM, Ferretti S, Monahan JE, Wang Y, Singh M, et al. High-throughput screening using patient-derived tumor xenografts to predict clinical trial drug response. Nature medicine. 2015; 21(11):1318–1325.
41. Itoh N, Ohta H. Fgf10: a paracrine-signaling molecule in development, disease, and regenerative medicine. Current molecular medicine. 2014; 14(4):504–509. [PubMed: 24730525]
42. Zhang X, Martinez D, Koledova Z, Qiao G, Streuli CH, Lu P. FGF ligands of the postnatal mammary stroma regulate distinct aspects of epithelial morphogenesis. Development (Cambridge, England). 2014; 141(17):3352–3362.
43. Piston DW, Kremers GJ. Fluorescent protein FRET: the good, the bad and the ugly. Trends in biochemical sciences. 2007; 32(9):407–414. [PubMed: 17764955]
44. Jozwik KM, Carroll JS. Pioneer factors in hormone-dependent cancers. Nature reviews Cancer. 2012; 12(6):381–385. [PubMed: 22555282]
45. Lasham A, Print CG, Woolley AG, Dunn SE, Braithwaite AW. YB-1: oncoprotein, prognostic marker and therapeutic target? The Biochemical journal. 2013; 449(1):11–23. [PubMed: 23216250]
46. EBCTCG. Effects of chemotherapy and hormonal therapy for early breast cancer on recurrence and 15-year survival: an overview of the randomised trials. Lancet (London, England). 2005; 365(9472):1687–1717.
47. Piasecka D, Kitowska K, Czaplinska D, Mieczkowski K, Mieszkowska M, Turczyk L, et al. Fibroblast growth factor signalling induces loss of progesterone receptor in breast cancer cells. Oncotarget. 2016; 7(52):86011–86025. [PubMed: 27852068]
48. Czaplinska D, Turczyk L, Grudowska A, Mieszkowska M, Lipinska AD, Skladanowski AC, et al. Phosphorylation of RSK2 at Tyr529 by FGFR2-p38 enhances human mammary epithelial cells migration. Biochimica et biophysica acta. 2014; 1843(11):2461–2470. [PubMed: 25014166]
49. Stratford AL, Reipas K, Hu K, Fotovati A, Brough R, Frankum J, et al. Targeting p90 ribosomal S6 kinase eliminates tumor-initiating cells by inactivating Y-box binding protein-1 in triple-negative breast cancers. Stem cells (Dayton, Ohio). 2012; 30(7):1338–1348.
50. Turner N, Lambros MB, Horlings HM, Pearson A, Sharpe R, Natrajan R, et al. Integrative molecular profiling of triple negative breast cancers identifies amplicon drivers and potential therapeutic targets. Oncogene. 2010; 29(14):2013–2023. [PubMed: 20101236]

51. Sharpe R, Pearson A, Herrera-Abreu MT, Johnson D, Mackay A, Welti JC, et al. FGFR signaling promotes the growth of triple-negative and basal-like breast cancer cell lines both in vitro and in vivo. Clinical cancer research : an official journal of the American Association for Cancer Research. 2011; 17(16):5275–5286. [PubMed: 21712446]

52. Chae YK, Ranganath K, Hammerman PS, Vaklavas C, Mohindra N, Kalyan A, et al. Inhibition of the fibroblast growth factor receptor (FGFR) pathway: the current landscape and barriers to clinical application. Oncotarget. 2016

53. De Luca A, Frezzetti D, Gallo M, Normanno N. FGFR-targeted therapeutics for the treatment of breast cancer. Expert opinion on investigational drugs. 2017; 26(3):303–311. [PubMed: 28121208]

54. Turner N, Pearson A, Sharpe R, Lambros M, Geyer F, Lopez-Garcia MA, et al. FGFR1 amplification drives endocrine therapy resistance and is a therapeutic target in breast cancer. Cancer research. 2010; 70(5):2085–2094. [PubMed: 20179196]

55. Tomlinson DC, Knowles MA, Speirs V. Mechanisms of FGFR3 actions in endocrine resistant breast cancer. International journal of cancer. 2012; 130(12):2857–2866. [PubMed: 21792889]

56. Musolino A, Campone M, Neven P, Denduluri N, Barrios CH, Cortes J, et al. Phase II, randomized, placebo-controlled study of dovitinib in combination with fulvestrant in postmenopausal patients with HR+, HER2- breast cancer that had progressed during or after prior endocrine therapy. Breast cancer research: BCR. 2017; 19(1):18. [PubMed: 28183331]

57. Curtis C, Shah SP, Chin SF, Turashvili G, Rueda OM, Dunning MJ, et al. The genomic and transcriptomic architecture of 2,000 breast tumours reveals novel subgroups. Nature. 2012; 486(7403):346–352. [PubMed: 22522925]

Europe PMC Funders Author Manuscripts

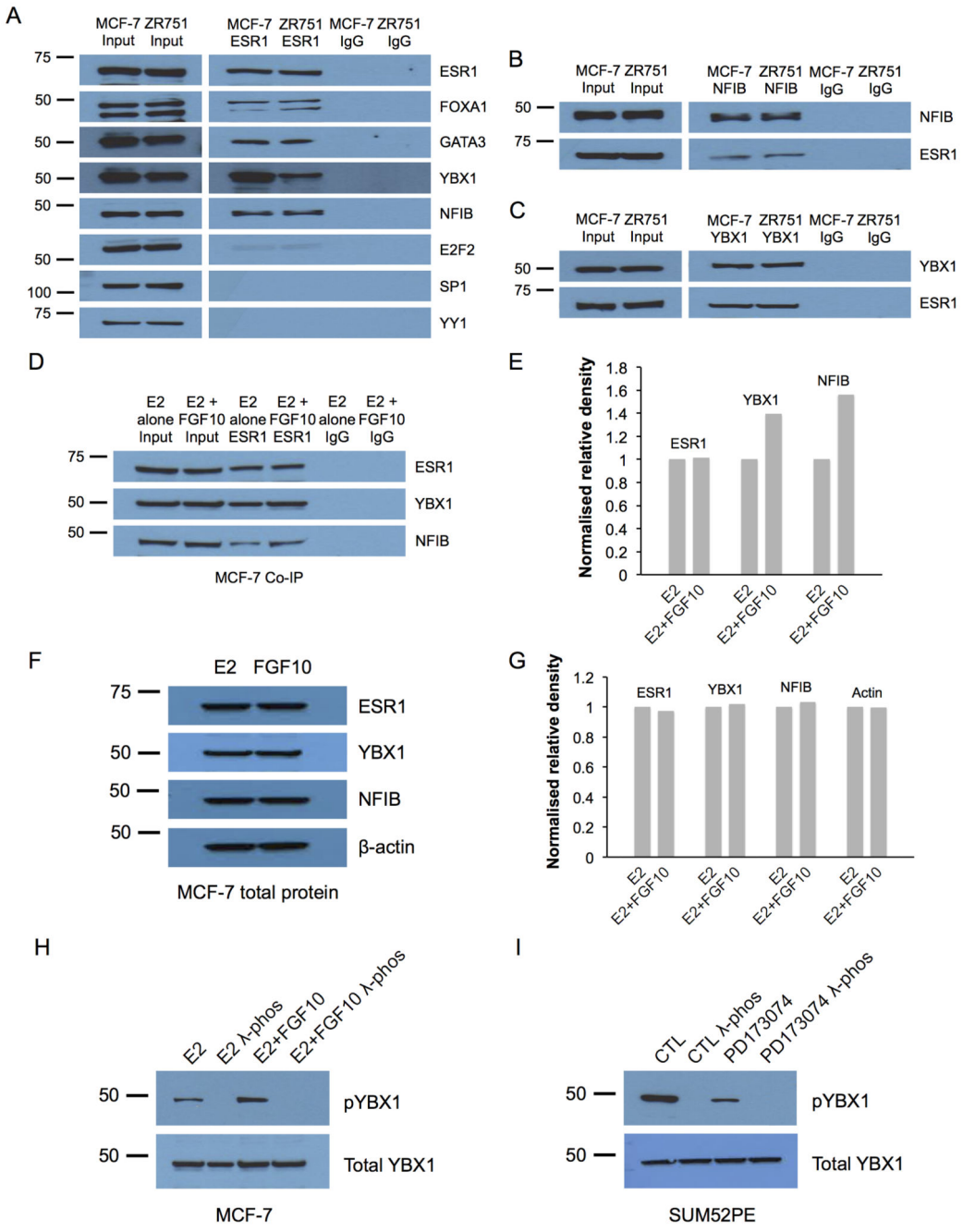

Figure 1.

ESR1 protein binds to the TFs NFIB and YBX1 in ER$^+$ breast cancer cells. (A-C) Co-immunoprecipitation assays were performed in MCF-7 and ZR751 cells, as indicated. Antibodies used in each immunoprecipitation are shown above the panels, antibodies used to develop Western immunoblots to the right of each panel. (D) Co-immunoprecipitation assays carried out in MCF-7 cells following treatment of the cells with 1 nM E2 or 1 nM E2 plus 100 ng/mL FGF10 for 90 minutes. (E) Densitometry analysis of the Western immunoblots displayed in D. (F) Representative Western immunoblots showing expression

Europe PMC Funders Author Manuscripts

of ESR1, NFIB, YBX1 and β-actin proteins in MCF-7 cells following treatment of the cells with E2 or E2 plus FGF10 (as above). (G) Densitometry analysis of the Western immunoblots displayed in F. (H) Representative Western immunoblots showing expression of phosphorylated YBX1 (pYBX1) and total YBX1 in MCF-7 cells following treatment of the cells with E2 or E2 plus FGF10 (as above). (I) Representative Western immunoblots showing expression of pYBX1 and total YBX1 in SUM52PE cells (carrying an FGFR2 gene amplification) following treatment of the cells with 100 ng/mL PD173074 (FGFR inhibitor) for 90 minutes. λ-phosphatase treatment of cell lysates was performed to demonstrate antibody specificity for phosphorylated (Ser102) YBX1. n=3 for all blots.

Europe PMC Funders Author Manuscripts

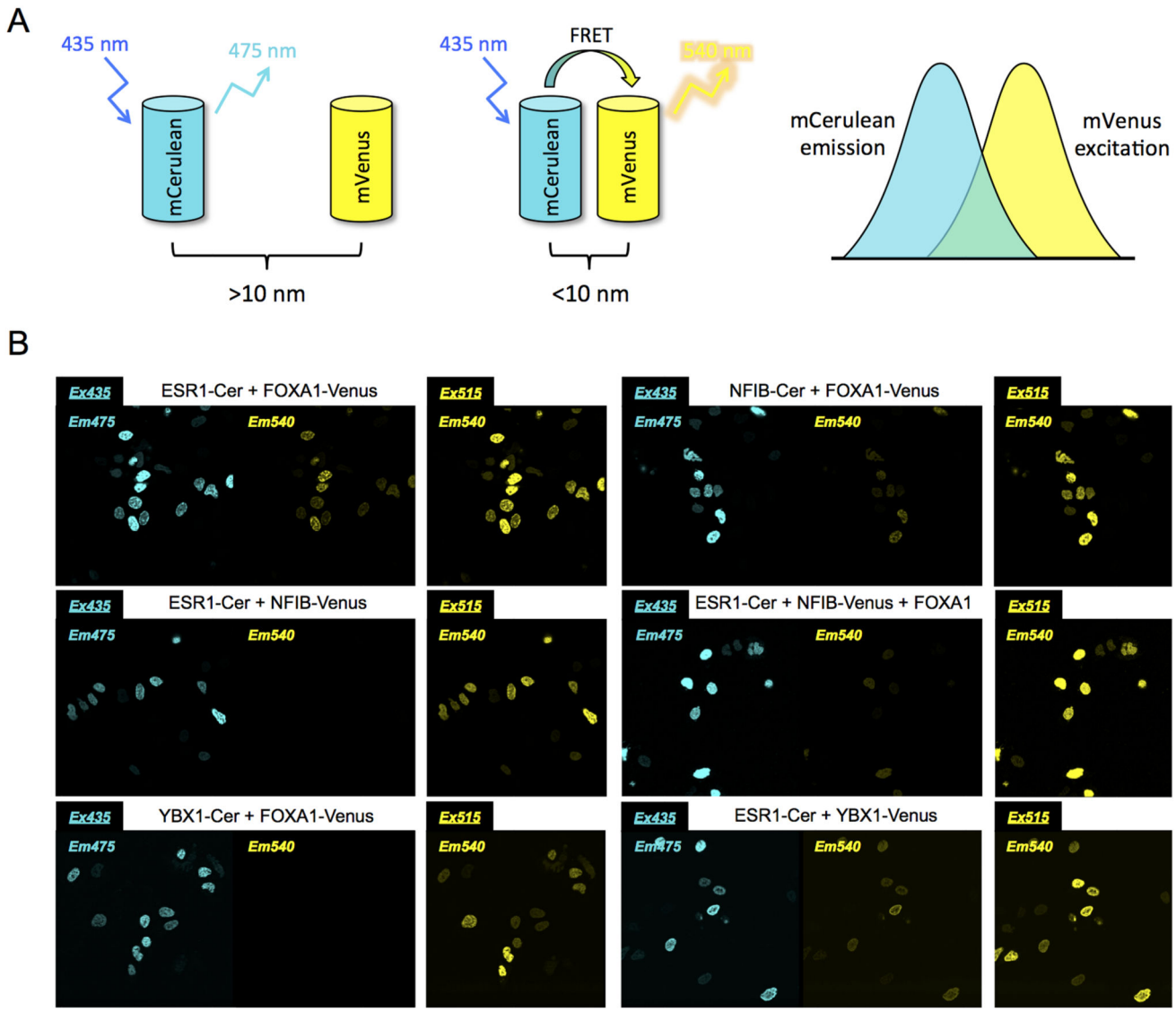

Figure 2.

FRET demonstrates protein-protein interactions between ESR1 and NFIB/YBX1. (A) Schematic showing how FRET microscopy works. If the FRET donor and acceptor fluorophores are >10 nm apart no FRET occurs and donor fluorescence is observed. If the FRET donor and acceptor fluorophores are within ~10 nm of one another, then energy transfer can occur from the donor to the acceptor. After excitation at 435 nm (Cerulean excitation), fluorescence at 540 nm (Venus emission) is only observed if the two FRET fluorophores are in very close proximity to one another (<10 nm), owing to the spectral overlap of the two fluorophores. (B) Representative images of FRET in HeLa cells transfected with FRET constructs, as listed above the panels. As expected, ESR1 and FOXA1 interact. FOXA1 also interacts with NFIB and facilitates the association of NFIB with ESR1. YBX1 interacts directly with ESR1 without interacting with FOXA1.

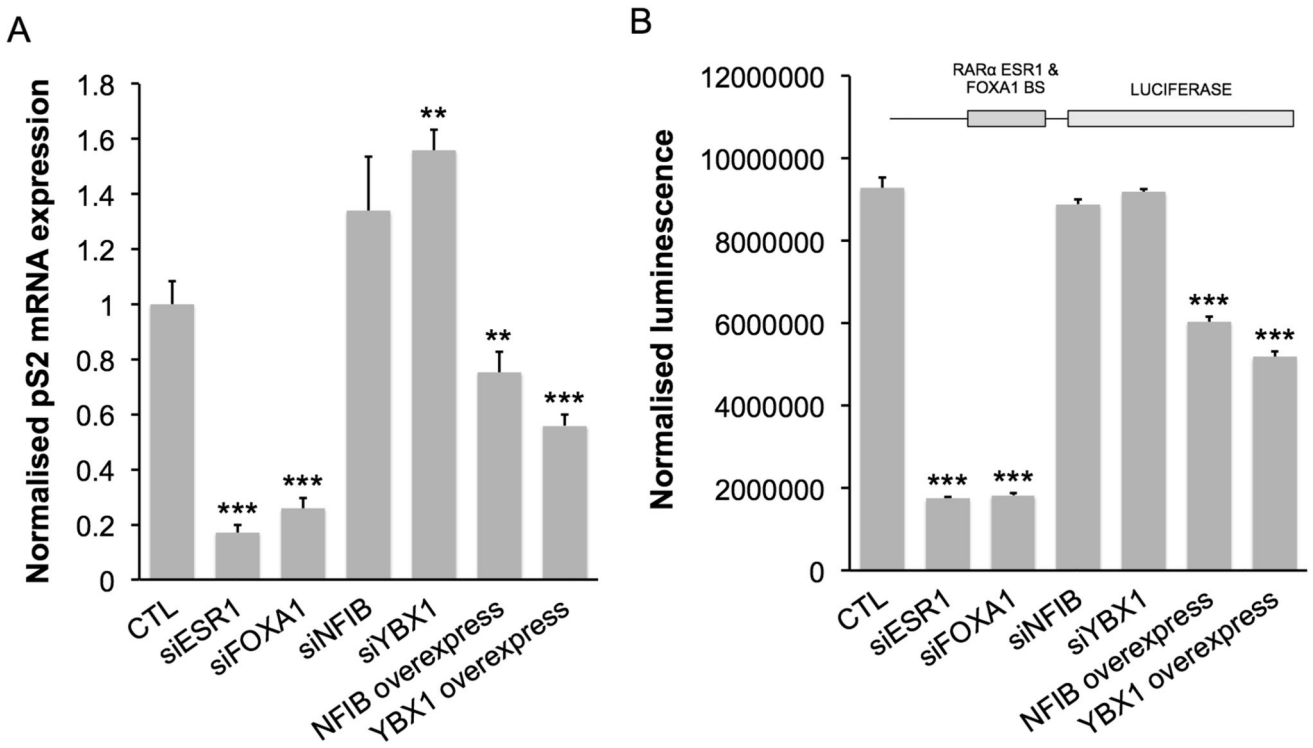

Figure 3.

NFIB and YBX1 repress the transcriptional activity of ESR1. (A) Relative mRNA expression of the ESR1-target gene, pS2, in MCF-7 breast cancer cells following transfection with siRNA directed against ESR1, FOXA1, NFIB and YBX1, and with plasmids overexpressing NFIB and YBX1, compared with a scrambled control siRNA transfection (CTL). All data were normalised to DGUOK expression (n=10, two separate experiments, P<0.01 (**), P<0.001 (***), one-way ANOVA and SNK correction, error bars = SEM). (B) Luciferase luminescence in MCF-7 cells stably expressing a luciferase reporter gene under the transcriptional control of an upstream ESR1/FOXA1 binding site, cloned from the human RARα gene, 24 hours post-transfection with siRNA directed against ESR1, FOXA1, NFIB and YBX1, and with plasmids overexpressing NFIB and YBX1, compared with a scrambled control siRNA transfection (CTL), normalised to β-galactosidase expression (n=9, three separate experiments, P<0.001 (***), one-way ANOVA and SNK correction, error bars = SEM). Inset: schematic depiction of the stably-expressed reporter construct used in the luciferase reporter assays.

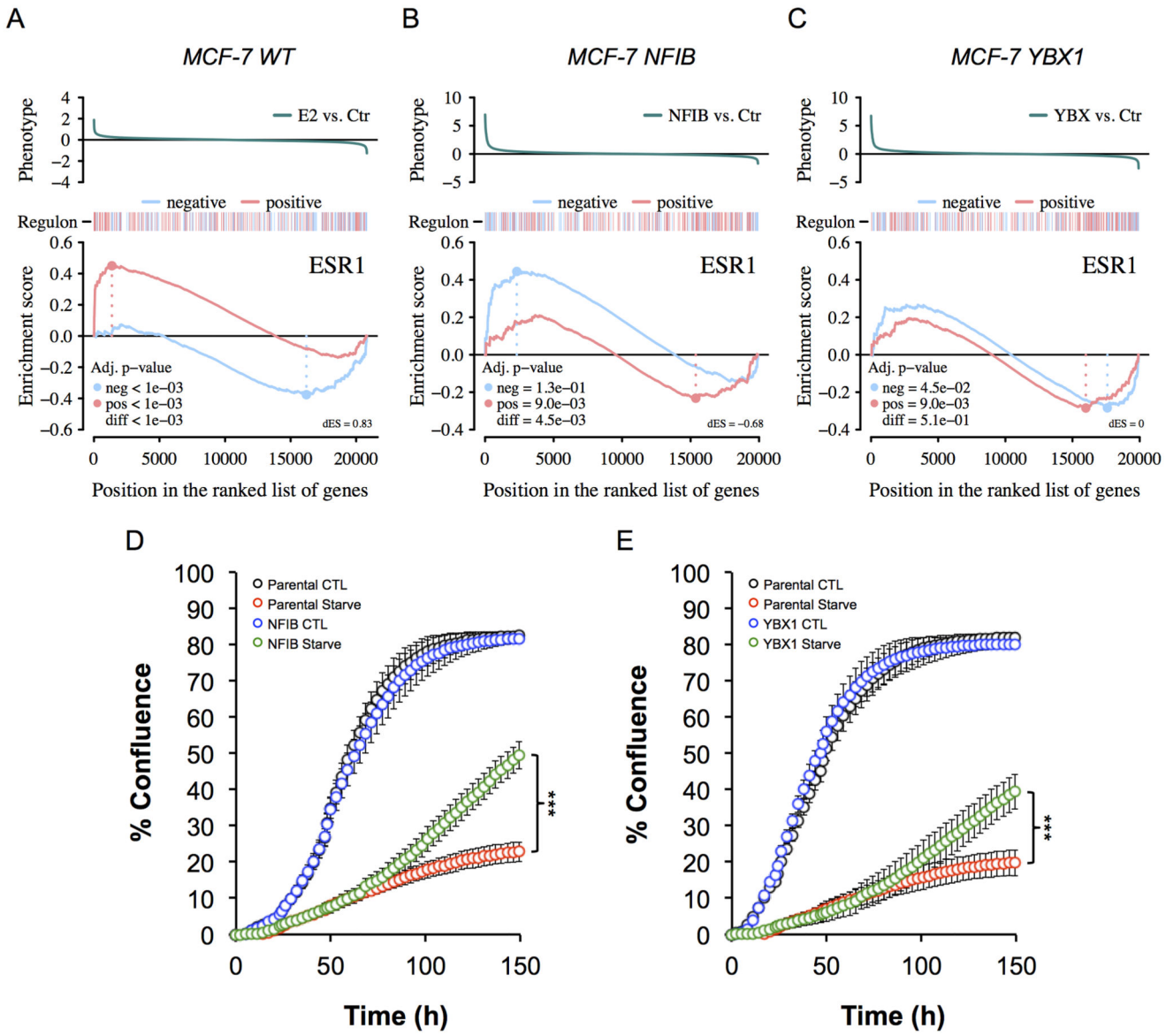

Figure 4.

Effect of overexpressing NFIB and YBX1 on the estrogen response. (A-C) GSEA of the ESR1 regulon using gene signatures derived from starved and estrogen-stimulated parental MCF-7 cells (A) and MCF-7 cells stably overexpressing NFIB (B) or YBX1 (C). (D,E) Effect of NFIB (D) and YBX1 (E) overexpression on MCF-7 cell proliferation in the absence of estrogen (n=16, two separate experiments, P<0.001 (***), one-way ANOVA and SNK correction, error bars = SEM).

Europe PMC Funders Author Manuscripts

Europe PMC Funders Author Manuscripts

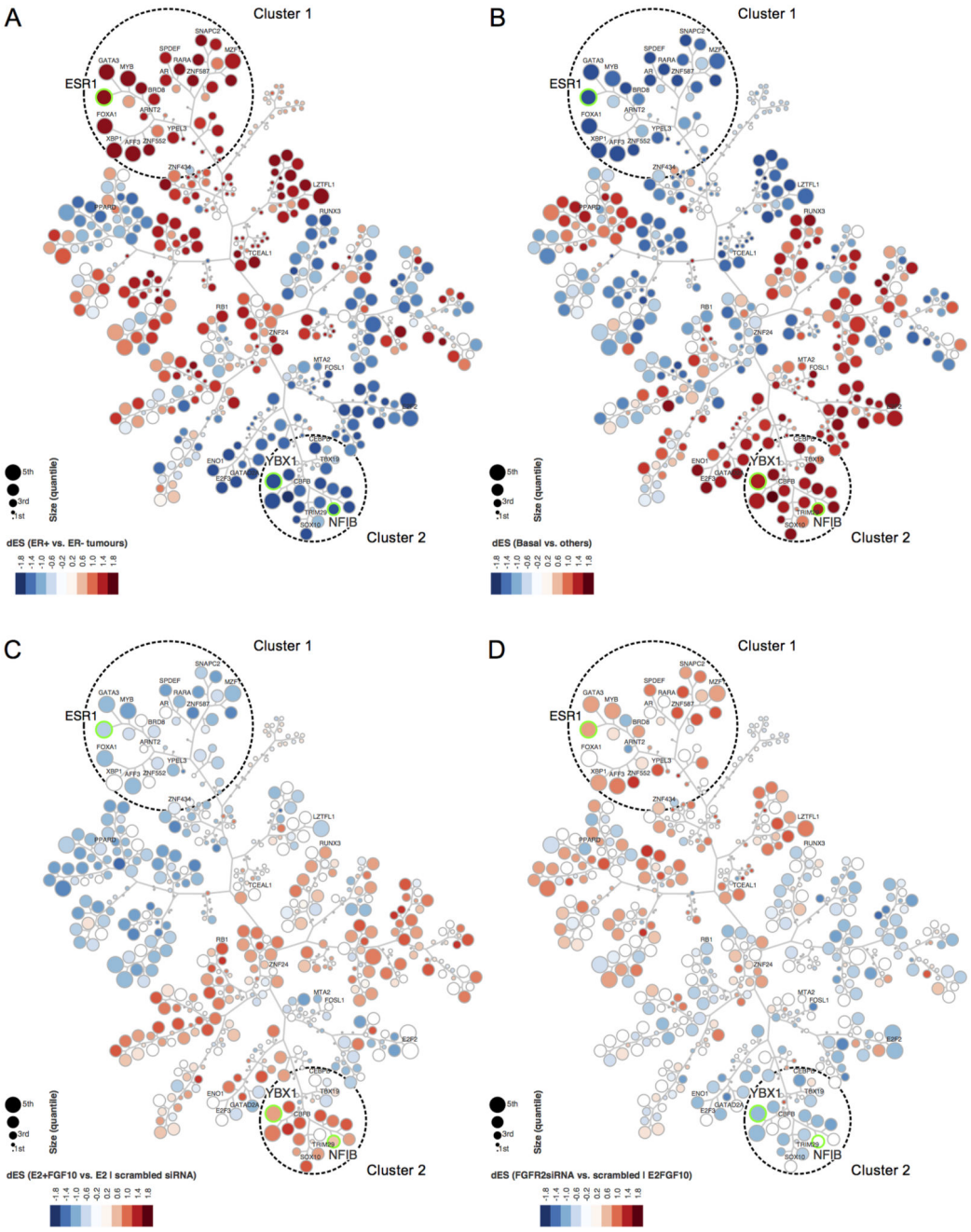

Figure 5.

FGFR2 signalling and breast cancer regulon activity. Tree-and-leaf representations of breast cancer regulon activity in ER^+ versus ER^- tumours (A), in basal versus non-basal tumours (B), in MCF-7 cells stimulated with FGF10 versus non-treated cells (C), and in MCF-7 cells transfected with siRNA directed against FGFR2 versus MCF-7 cells transfected with a non-targeting control siRNA (D). Generation of the tree-and-leaf diagrams, representing the breast cancer risk TF network, has been described previously [5]. The size of the regulons is represented by circle size, and differential enrichment score (dES), as determined by GSEA,

is represented by colour. Data for A and B were from the METABRIC data set [57]. Data for C and D were from microarray analysis (deposited in GEO under the SuperSeries number GSE74663).

Europe PMC Funders Author Manuscripts

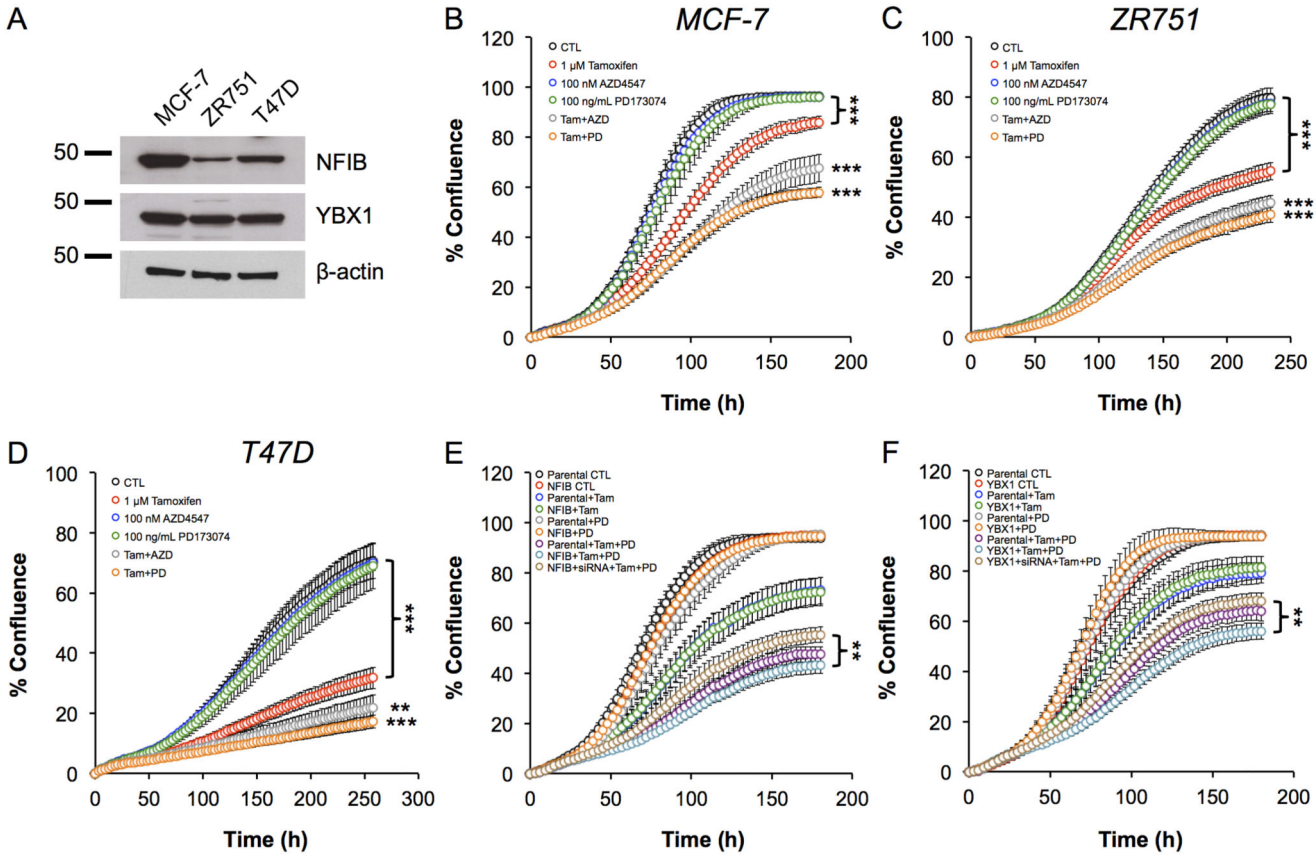

Figure 6.

FGFR2 inhibition sensitizes ER$^+$ breast cancer cells to anti-estrogen therapies. (A) Representative Western immunoblots showing expression of NFIB, YBX1 and β-actin proteins in MCF-7, ZR751 and T47D cells (n=3 for all blots). (B-D) Growth curves for MCF-7 (B), ZR751 (C) and T47D (D) cells following treatment with 1 μM tamoxifen, 100 nM AZD4547 (FGFR inhibitor), 100 ng/mL PD173074 (FGFR inhibitor), 1 μM tamoxifen plus 100 nM AZD4547 (Tam+AZD) or 1 μM tamoxifen plus 100 ng/mL PD173074 (Tam +PD). (E,F) Growth curves for parental MCF-7 cells versus MCF-7 cells stably overexpressing NFIB (E) or YBX1 (F) following treatment with 1 μM tamoxifen (Tam), 100 ng/mL PD173074 (PD), 1 μM tamoxifen plus 100 ng/mL PD173074 (Tam+PD) or siRNA directed against NFIB (E)/YBX1 (F) plus 1 μM tamoxifen plus 100 ng/mL PD173074 (siRNA+Tam+PD). n=16 for all growth curves, two separate experiments, P<0.01 (**), P<0.001 (***), one-way ANOVA and SNK correction, error bars = SEM. Statistical comparison for the Tam+AZD/PD treatments in panels B-D is against the tamoxifen alone treatment shown in red. To avoid overlapping curves in panels E and F, data from parental and stably expressing cell lines are presented separately in Supplementary Figure 5.

Europe PMC Funders Author Manuscripts

Table 1

RIME analysis shows ESR1 binds to NFIB and YBX1.

	E2		*E2+FGF10*		*IgG*	
	ZR751	**MCF-7**	**ZR751**	**MCF-7**	**ZR751**	**MCF-7**
ESR1	8	8	7	7	0	0
GATA3	3	3	2	3	0	0
FOXA1	1	1	1	0	0	0
NFIB	1	0	1	2	0	0
YBX1	2	4	4	7	0	1

Values indicate the number of unique peptides identified by MS for the TFs listed in the left column, in ZR751 and MCF-7 ER^+ breast cancer cells, following nuclear immunoprecipitation with an ESR1 antibody after treatment with 1 nM E2 or 1 nM E2 plus 100 ng/mL FGF10 (E2+FGF10) for 90 minutes, or with an IgG control antibody after E2 treatment.